ADVANCED CHARACTERIZATION OF NON-CONVENTIONAL BIOMASS (FROM EMERGING MARKETS) IN A FIXED-BED REACTOR

A. Rezeau[1], J. Royo[2], J. Ribas[3], A. Masot[3], M. Díaz[1], S. Sala[1] and N. Yescas[4]
[1] CIRCE – Research Centre for Energy Resources and Consumption, Zaragoza, Spain
[2] University of Zaragoza, Department of Thermal Machines and Motors, Zaragoza, Spain
[3] L.Solé S.A., Biomass Solutions Company, Mataró, Spain
[4] Monterrey Institute of Technology and Higher Education, Monterrey, Mexico

ABSTRACT: This work presents the first results of non-conventional biomass characterization in a fixed bed reactor. The lab-scale device consists in a cylindrical tube of 1700 mm height and 200 mm diameter, made of stainless steel and insulated with ceramic and wool fibers. Measurements of temperature along the bed height, as well as reactor mass loss and gaseous emissions at the outlet have been performed and have allowed determining the velocity of the ignition front propagation, the mass ignition rate and the temperature of the reaction front. Experimental tests have been carried out with rice husks and compared two standardized woody fuels, one pelletized and one chipped. The results show that the behavior of the non-conventional fuel differ substantially from the woody biomass. In particular, the physical properties of the rice husk seem to mostly influence its conversion behavior, *i.e.*, a very high ignition front propagation velocity and high mass ignition rate. In the next future, tests with additional non-conventional biomasses will be carried out and the results will be used to derive data for designing and optimizing the operation of a large-scale grate-fired unit, *e.g.*, optimum primary air flow under each grate section, adjusted grate velocity, etc.
Keywords: batch reactor, combustion, fixed bed, rice husk, reactivity, emissions.

1 INTRODUCTION

Small scale fixed bed reactors have been utilized in numerous occasions to investigate the conversion of solid fuels (*e.g.*, biomass or wastes) and to simulate the process that takes place in real grate-fired devices. The purpose of these works was mainly related to the characterization of the ignition front propagation [1-4], but also to study the effect of staged combustion on NO_X emissions [5-6] or the effects of operating conditions on particle emissions [7].

The present work is framed in a R&D project between a biomass boiler manufacturer, L.Solé, and a research center, CIRCE, which aim is to adapt the current combustion technology to the complex characteristics of non-conventional biomasses, such as grape pomace, rice husk, king grass or maize corn. Although these feedstocks present high potential, especially in emerging markets (e.g., Central America or Asia), they are not always valorized due to their difficult conversion in the current grate-fired biomass boilers. This may be mainly explained because they present high ash content, high content of problematic elements (Si, K, etc.), water content variability and/or wide range of particle size (including high content of fines).

To reach that goal, L.Solé and CIRCE have designed and constructed a fixed bed reactor able to characterize the conversion of these problematic fuels under determined combustion conditions. In particular, the reactor allows investigating the characteristics of the ignition front propagation and the gaseous emissions that are obtained for a specific fuel under different primary air conditions. Based on the results of the lab-scale reactor and, especially, the comparison between the behavior of conventional vs. non-conventional fuels, relevant data can be derived and will support the adaptation and the improvement of the new grate-fired boiler design and operation.

In this paper, an advance of the characterization results with this reactor is presented and correspond to three different fuels. The first two are woody stem-based fuels that are pelletized or chipped and the third fuel consists in rice husks. This biomass is a very abundant agro-industrial residue in Latin America, but presents a complex combustion behavior due to a very low bulk density, a high ash content and a high tendency to form slag.

2 METHODOLOGY

2.1 Properties of the studied fuels

Three different biomass types have been evaluated in this work: pine pellets (PP), pine chips (PC) and rice husk (RH). Other fuels such as king grass (fast growing grass), grape pomace and corn cob are also under study but not included in this paper.

Main fuel characteristics are presented in Table I and a photograph of PC and RH is depicted in Fig. 1.

Figure 1: Photograph of the rice husks (RH) and the pine chips (PC), tested for the present work.

As it is shown in Table I, RH presents the lowest energy density. This fuel is also the one with the highest ash content (A) and the lowest volatiles-to-fixed carbon ratio (V/FC). These properties suggest that specific combustion conditions are required compared to the conventional fuels (PP and PC) for a satisfactory combustion. For instance, it is expected that a higher amount of air will be needed based on the V/FC ratio results.

Concerning ash composition, it is shown that main ash forming elements are: Ca, Mg, Si, P and K. Additionally, a high Al content was obtained for the RH fuel, which may suggest soil contamination. Based on the main ash elements, it can be expected melting tendency of ashes to form slag, particularly for RH.

This fact is supported by fusibility temperature results. As presented in Table I, the woody fuels have high melting temperature, whereas RH has an initial deformation temperature close to 1200ºC, which is a typical grate-combustion condition.

Table I: Properties of the studied fuels

	PP	PC	RH
ρ_{bulk}, kg/m^3	690	270	114
LHV, MJ/kg a.r.	17,55	15,07	13,59
Proximate analysis			
W, wt% a.r.	7,20	17,19	11,87
A, wt% d.b.	0,29	0,96	15,96
V/FC	6,28	5,47	4,49
Ultimate analysis (% wt, d.a.f.)			
C	51,10	49,94	49,35
H	6,12	5,92	6,13
N	0,09	0,10	0,86
S	0,00	0,02	0,08
Cl	0,01	0,01	0,08
O*	42,66	44,02	43,5
Ash composition (mg/kg fuel, d.b.)			
Al	-	25,0	129,1
Ba	-	0,0	3,0
Ca	-	1793,0	910,4
Fe	-	77,9	153,1
Mg	-	240,4	545,3
P	-	505,7	404,2
K	-	377,8	1989,9
Si	-	9,6	51855,9
Na	-	10,6	294,1
Ti	-	13,5	2612,2
Fusibility temperatures (ºC)			
IDT	>1400	>1500	1198
ST	>1400	>1500	1359
HT	>1400	>1500	1426
FT	>1400	>1500	1485

***** By difference

Finally, size distribution has been performed with PC and RH, according to the corresponding norm (EN 15149-3). The results indicate that RH has its predominant fraction for sizes comprised between 1 and 3 mm, meanwhile PC predominant fraction equals to 3 – 16 mm.

2.2 Experimental Facility

A fixed bed reactor has been specifically designed and constructed for this work. It consists of a vertical cylindrical combustor chamber, a grate, the air supply system, a flue gas analyzer and a weighing scale, as shown in Fig. 2. The chamber is made of stainless steel AISI-310S having a height of 1.7 m, an inner diameter of 200 mm and 8 mm thick. The insulating around the side wall is made of two different materials: ceramic fiber (50 mm) and rockwool (70 mm). Fifteen thermocouples are inserted along the chamber wall; five of them in the freeboard (each 15 cm) and the others ten are located within fuel bed (each 5 cm).

Air is supplied from the bottom of the arrangement, through the grate and the fuel bed, providing an adequate distribution over the whole transverse area. In addition, a hot-wire anemometer measures the air flowrate continuously and sends the signal to PID controller for adjusting the frequency of the fan. The reactor is suspended from a weighting scale that allows monitoring the mass loss of the fuel bed. All the measured data (temperatures, reactor weight and air flowrate) are registered, for every 10 or 2 s, depending on the fuel that is burnt. In addition, a gas analyzer MRU SYNGAS continuously measures O_2, CO, CO_2, NO, NO_2, SO_2 and CH_4 concentrations, at the reactor outlet. Before the gas escape to the atmosphere, a metallic filter is in charge of collecting the coarse fraction of the fly ashes, so they can be quantified and analyzed. Finally, it is interesting to underline that the ignitor can be inserted in three different levels, depending on the type of fuel charged in the reactor: 200, 350 or 500 mm.

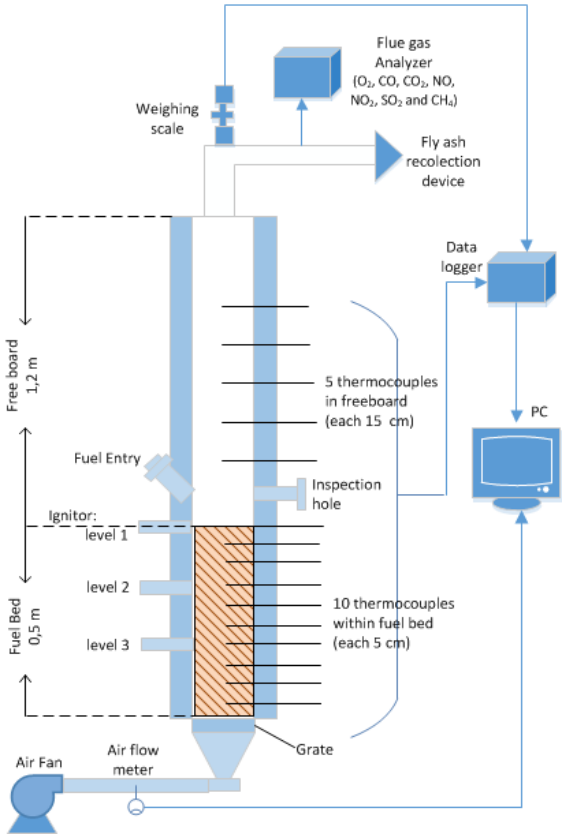

Figure 2: Scheme of the experimental test facility

2.3 Calculated data

Thermocouples are used in this plant to measure the bed temperature at different levels and thus to provide the velocity of the ignition front propagation. The time taken to reach a specific predetermined temperature (500ºC in this work) between two adjacent thermocouples enables the front propagation velocity to be calculated, in mm/s.

The mass ignition rate, *i.e.*, the amount of ignited mass per unit time per unit surface area (in kg/m^{2}s) is obtained by multiplying the ignition velocity per the bulk density of the fuel.

In addition, the thermocouples allow determining the reaction front temperature for a determined fuel and air conditions, *i.e.*, the mean of the maximum temperatures measured by each thermocouple inserted in the fuel bed.

Finally, the stoichiometry of the reaction may be determined after each test by the following equation [3]:

$$\lambda = \frac{m_{air}}{AF_{stq} * m_{ir}}$$

where m_{air} is the mass flowrate of primary air injected (kg/m^{2}s), m_{ir} is the mass ignition rate (kg/m^{2}s) and AF_{stq} the stoichiometric air-to-fuel ratio of the studied biomass.

3 RESULTS AND DISCUSSION

In this section, results obtained during the first tests in the lab-scale reactor are described. In total, a set of 51 tests have been carried out, which correspond to the variation of two main parameters: the fuel (PP, PC and RH) and the mass flow of primary air. Several tests have been performed at each tested condition, for repeatability, and the average of the measured parameter (e.g., mass ignition rate) is depicted in the next figures. Comparison is made between the three tested fuels in terms of ignition front velocity, mass ignition rate, temperature of the reaction front and gaseous emissions at reactor outlet.

3.1 Ignition front velocity

As can be seen in Fig. 3, the velocity of the ignition front propagation varied substantially among the tested fuels. The lowest velocity has been found for the pelletised fuel (PP), while the highest velocity has been obtained for the RH. In that case, ignition front velocity was almost ten times higher than the one obtained for PP. This can be partly explained by the important difference in the bulk density of both fuels, *i.e.*, 114 kg/m^3 for the RH and 690 kg/m^3 for the PP, as well as the very small particle size of the RH (between 1 and 3 mm).

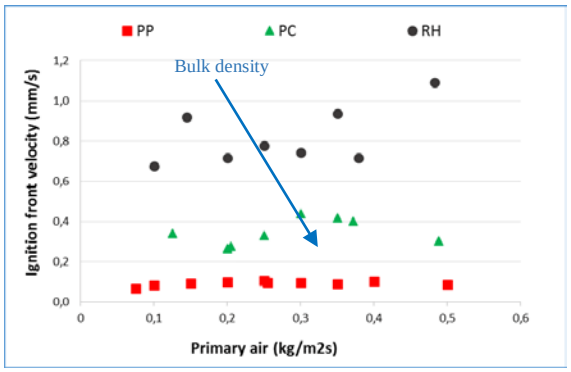

Figure 3: Ignition front velocity vs. primary air flowrate, for the three tested fuels (PP, PC and RH).

3.2 Mass ignition rate

The mass ignition rate can be determined, for each test, by multiplying the front velocity per the bulk density of the tested fuel. As can be seen in Fig. 4, PP and PC present a similar tendency, *i.e.*, a "dome" curve, although absolute values differ substantially.

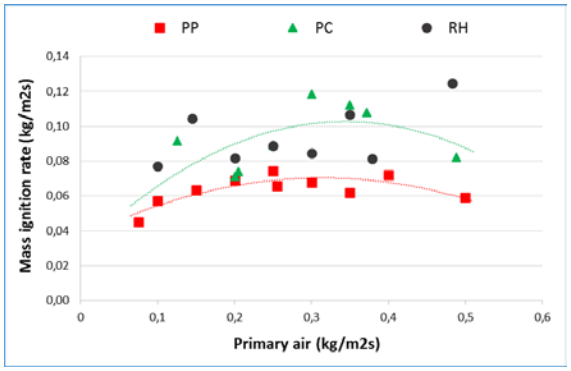

Figure 4: Mass ignition rate vs. air flowrate, for the three tested fuels (PP, PC and RH).

For both fuels, it may be clearly seen that the mass ignition rate decreases as primary airflow decreases, due to a lack of oxygen. At these fuel-rich conditions, the temperatures' profiles and the mass loss curve indicated two distinct regimes, as it can be seen in Fig. 5. In this graph, it can be observed how the flame propagates along the bed height during the first part of the test, with relatively low bed temperatures (< 800ºC). Then, when the ignition front arrives at the grate level (see sensor_1 in Fig. 5), temperatures increase quickly up to approximately 1300ºC and, on the contrary, the mass loss rate decreases substantially. This may be explained because at fuel-rich conditions the char is produced at a higher rate than its consumption rate. Only when ignition has ended, the available oxygen can be consumed for char reactions, which corresponds to the second part of the test (high temperature and low mass loss rate).

On the other hand, it may be observed in Fig. 4 that when air flowrate is high (above 0,4 kg/m^{2}s), mass ignition rate decreases again, for PP and PC, due to the convection of the primary air flow that cools down the reactions in the fuel bed.

Concerning RH, the behavior differs greatly from woody biomass and the results depicted in Fig. 4 do not allow identifying a clear tendency for this non-conventional fuel. Even so, the temperature profiles obtained during tests with RH show that its conversion behavior is mostly affected by the air flowrate applied. Firstly, two different regimes are observed during tests at low air flowrates (≤ 0,25 kg/m^{2}s), see Fig. 6, as it was detected for PC (in Fig. 5).

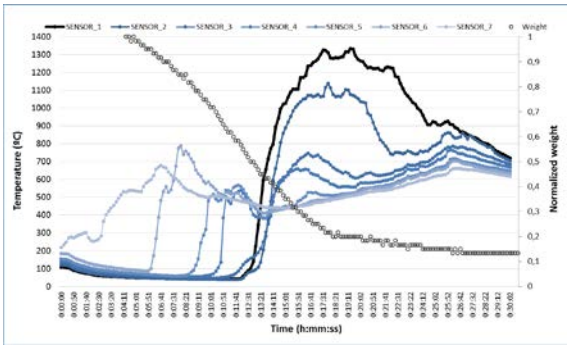

Figure 5: Profiles of temperature within the bed (thermocouples 1 to 7) and mass loss, during test with PC and low airflow rate (0,125 kg/m^{2}s).

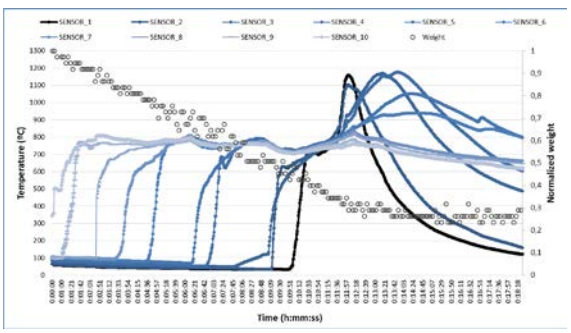

Figure 6: Profiles of temperature within the bed (thermocouples 1 to 10) and mass loss, during test with RH and low airflow rate (0,2 kg/m^{2}s).

Secondly, the temperature profile illustrated in Fig. 7 shows that when the air flowrate reaches intermediate values (i.e., 0,3-0,4 kg/m2s), the behavior of RH becomes quite stable. Finally, it is interesting to stress out that both the ignition time and the shut-off time were very fasts during tests with RH, as it can be seen in Fig. 6 and 7.

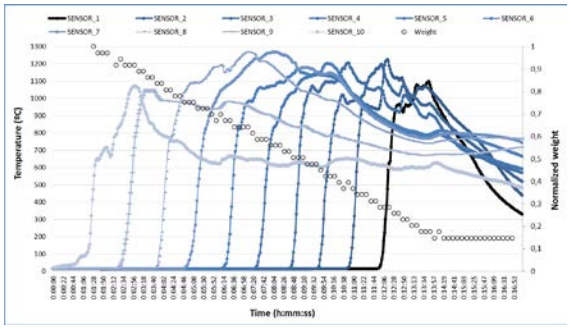

Figure 7: Profiles of temperature within the bed (thermocouples 1 to 10) and mass loss, during test with RH and intermediate airflow rate (0,3 kg/m^{2}s).

3.3 Reaction front temperature

Fig. 8 is depicted in order to compare the reaction front temperature obtained for the different fuels as a function of the primary air flowrate injected. As can be seen, this parameter is very sensitive to air flowrate, for the three tested fuels. Moreover, the fuels behavior differs substantially, *i.e.*, the reaction front temperature decreases when air flowrate increases for RH while PP and PC show an opposite trend. Notwithstanding, it is necessary to carry out additional tests at higher air flowrate (e.g., above 0,5 kg/m^{2}s), for the three tested fuels.

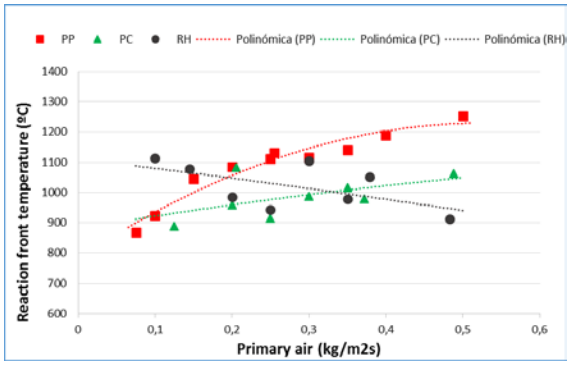

Figure 8: Temperature of the reaction front for the three tested fuels, as function of the primary air flowrate injected.

In order to gain insight into the behavior of each fuel, Fig. 9 is also given. There, the maximum temperature registered at a specific air flowrate and the temperature of the reaction front at the same condition are illustrated, for each fuel. As can be seen, both parameters follow the same tendency for the pelletized woody fuel (PP), *i.e.*, both temperatures increase as the air flowrate increases. In addition, the difference between these two parameters is low, with a mean of 70ºC for all tests. The maximum difference is found for test at lowest air flowrate (0,075 kg/m^{2}s) and it is equal to 150ºC. This fact may also be explained by the phenomenon that occur at fuel-rich conditions and that provokes a temperature peak at the end of the test, when all the fuel has been ignited and the char oxidation takes place.

Concerning PC, its behavior differs mostly from PP, as it can be observed in Figs. 8 and 9. For the chipped fuel, there exists a large difference between the maximum temperature and the temperature of the reaction front (~400ºC), at low air flowrates. Then, both parameters got closer as air flowrate increases. This phenomenon may be explained by the lack of oxygen at low air flowrates that creates two distinct regimes during the conversion process in the bed (see Fig. 5). There, a temperature peak takes place near the grate (sensor 1 up to 1300ºC) that correspond to char reactions but the rest of the thermocouples, and so the temperature of the reaction front, are quite low (<800ºC) during all the test duration. Also, the difference between PP and PC may be explained by the larger volatiles-to-f ratio in PP and therefore a lower tendency to produce char during its devolatilization.

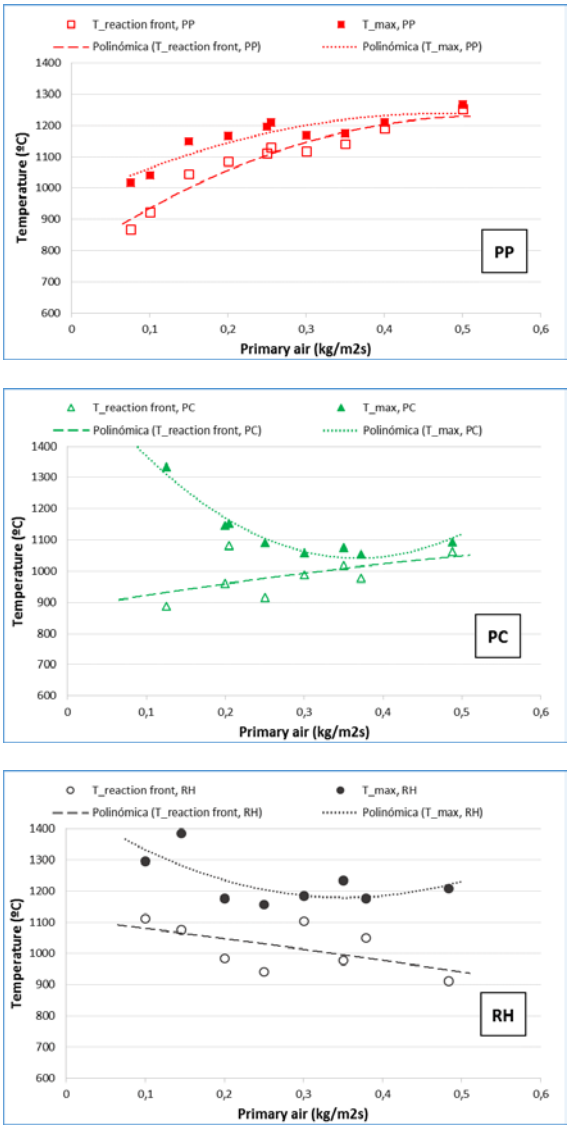

Figure 9: Comparison between the reaction front temperature and the maximum temperature registered for each test, as function of the air flowrate injected and the tested fuel.

Finally, the graph of the maximum and the reaction front temperatures for RH show that an increase of the primary air flowrate negatively affects these parameters. Contrary to what was obtained for PP and PC, the reaction front temperature decreases substantially as air flowrate increases. Besides, the difference between the maximum and the reaction front temperatures is almost constant among the tests and is relatively high, with an average around 190ºC. Although additional tests are needed, these results suggest a major effect of the convection cooling on this fuel.

3.4 Gaseous emissions

In this section, the effect of air flowrate on gaseous emissions during RH conversion is analyzed. For that aim, the concentrations of O_2, CO, CO_2 and CH_4 in dry gas are depicted in Fig. 10 to 12 and correspond to test with low, medium and high air flowrate, respectively.

By comparing the three graphs, it may be observed that primary air flowrate substantially influences the composition of the gas at the reactor outlet. Since the device does not account for a secondary air injection, the analyzed gas may be approximated to the gas that escapes from the fuel bed surface during the operation in a real grate-fired boiler.

Observing Fig. 10, at the lowest air flowrate, it may be seen that the gaseous emissions were unstable and presented high concentrations of gaseous unburnt (CO and CH_4). Concerning CO, it reached its highest concentration (13%) during the first part of the test (0:06:14). At the same time, CH_4 also reached very high values, i.e., up to 30000 ppm. The two decreases observed in this period may be due to a problem in the gas analyzed, which "shut down" when CH_4 concentration was above 30000 ppm. Also, it may be underlined that the last period of the test, when O_2 concentration increases again up to 21%, was much longer compared to test at intermediate air flowrate (see Fig. 11).

Concerning test at intermediate air flowrate, it can be observed in Fig. 11 that gaseous emissions were stable, with relatively low contents of unburnt. In that case, concentrations were respectively of 7,4%, 4% and 11% for O_2, CO and CO_2. With respect to CH_4, the highest peak was found at the beginning of the stable conversion phase, with a value of 4.000 ppm.

Finally, it may be seen in Fig. 12 that gaseous emissions were unstable again at high air flowrate condition. In this case, two large peaks of CO and CH_4 can be identified and correspond to the first period of the test.

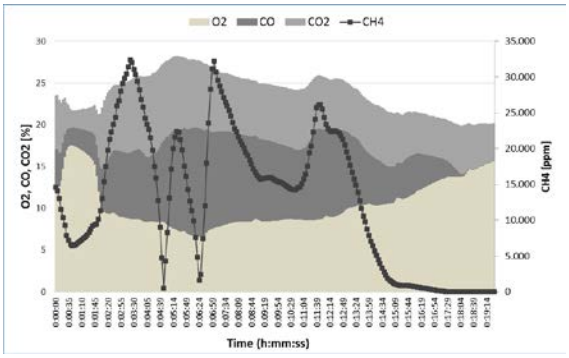

Figure 10: Gaseous emissions during conversion of RH at low air flowrate (0,1 kg/m^{2}s).

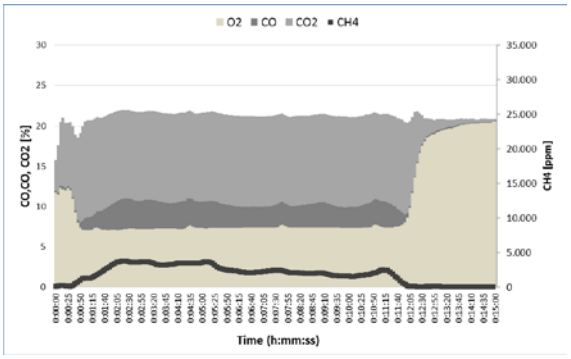

Figure 11: Gaseous emissions during conversion of RH at intermediate air flowrate (0,3 kg/m^{2}s).

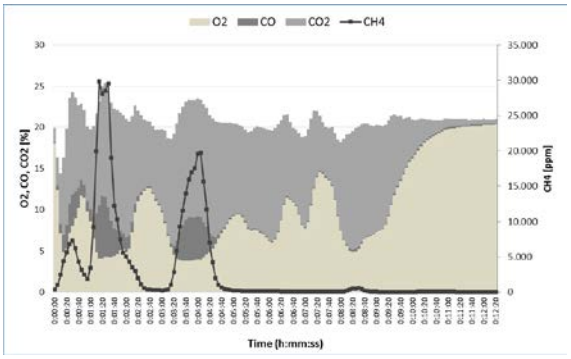

Figure 12: Gaseous emissions during conversion of RH at high air flowrate (0,5 kg/m^{2}s).

5 CONCLUSIONS AND FUTURE WORK

This work has presented the first results of non-conventional biomass characterization in a fixed bed reactor. Experimental tests were carried out with rice husks and compared two standardized woody fuels, one pelletized and one chipped. The results showed that although a strong effect of the air flowrate was detected on the conversion behavior of the three tested fuels, the results differ substantially between the non-conventional and the woody biomass. In particular:

- In the case of RH, a very high velocity of ignition front propagation was obtained, mainly due to the physical characteristics of the RH (small particle size and very low bulk density).
- Also, time for ignition and shut-down were very short for RH, in comparison to PP and PC.
- Concerning mass ignition rate, no clear tendency was found for the non-conventional fuel, and additional tests are needed, especially at high air flowrates (> 0,5 kg/m^{2}s).
- As regards the maximum temperature in the bed and the temperature of the reaction front, trends between RH and woody fuels were opposite. In the non-conventional fuel case, these parameters decreased as air flowrate increased and, in addition, the difference between both temperatures was quite important (~190ºC).

In the next future, tests with additional non-conventional biomasses (such as grape pomace, king grass or corn cobs) will be carried out. The results will be

used to derive data for designing and optimizing the operation of a large-scale grate-fired unit, *e.g.*, optimum primary air flow under each grate section, adjusted grate velocity, etc.

6 REFERENCES

[1] Ryu, C., et al., Effect of fuel properties on biomass combustion: Part I. Experiments—fuel type, equivalence ratio and particle size. Fuel, 2006. 85: p. 1039-1046.

[2] Porteiro, J., et al., Experimental analysis of the ignition front propagation of several biomass fuels in a fixed-bed combustor. Fuel, 2010. 89(1): p. 26-35.

[3] Porteiro, J., et al., Study of the reaction front thickness in a counter-current fixed-bed combustor of a pelletised biomass. Combustion and Flame, 2012. 159(3): p. 1296-1302.

[4] Horttanaimen, M.V.A., et al., Operational limits of ignition front propagation against airflow in packed beds of different wood fuels. Energy & Fuels, 2002. 16: p. 676-686.

[5] Houshfar, E., et al., Effect of Excess Air Ratio and Temperature on NOx Emission from Grate Combustion of Biomass in the Staged Air Combustion Scenario. Energy & Fuels, 2011. 25(10): p. 4643-4654.

[6] Houshfar, E., et al., NOx emission reduction by staged combustion in grate combustion of biomass fuels and fuel mixtures. Fuel, 2012. 98(0): p. 29-40.

[7] Wiinikka, H., et al., Critical Parameters for Particle Emissions in Small-Scale Fixed-Bed Combustion of Wood Pellets. Energy & Fuels, 2004. 18(4): p. 897-907.

7 NOMENCLATURE

Acronyms

FC	Fixed Carbon
FT	Fluid Temperature
HT	Hemisphere Temperature
IDT	Initial Deformation Temperature
LHV	Low Heating Value
PC	Pine Chips
PP	Pine Pellet
RH	Rice Husk
ST	Softening Temperature

Roman symbols

A	Ash content [%, d.b.]
W	Water content [%, a.r.]

Greek symbols

ρ_{bulk}	Bulk density [kg/m^3 a.r.]

8 ACKNOWLEDGEMENTS

The authors are grateful to the Spanish Ministry of Economy and Competitiveness for funding the project HBE "New furnace for the efficient conversion of non-conventional biomass (from emerging market)", ref. RTC-2014-2719-3

9 LOGO SPACE